Journal of Applied Mechanics Vol.8, pp.171-178 (August 2005) JSCE

An efficient method for computation of singular and higher order terms of a crack-tip stress field

亀裂先端近傍応力場に関する高次項の効果的な算出法

Santosh Shrestha * and Mitao Ohga **
シュレスタ サントシュ・大賀水田生

*Member, Graduate student, Dept. of Civil & Envn. Eng., Ehime University, Bunkyo-cho 3, Matsuyama 790-8577
** Member, Dr. of Eng., Professor, Dept. of Civil & Envn. Eng., Ehime University, Bunkyo-cho 3, Matsuyama 790-8577

A recently developed semi-analytical method, called scaled boundary finite element method, is applied to evaluate the coefficients of stress field at a crack-tip for two-dimensional linear-elastic cracked structures. The method has ability to analytically compute stress and displacement field of singularities region at the crack-tip more accurately without any *a priori* assumptions. A simple and independent formulations for evaluating the coefficients, not only of the inverse square root singular term but also of the constant and higher order non-singular terms, of the stress fields near crack-tip is presented by comparing the stress along the radial points ahead of the crack-tip with that of standard Williams' eigenfunction solution for the crack-tip. The accuracy and efficiency of the formulations are examined by numerical examples for a range of crack sizes. The results are in agreement with available solutions in literatures

Key Words: *stress field near a crack-tip, SIFs, T-stress, higher order terms, scaled boundary finite element method*

1. Introduction

Failure of a structure is often a result of a complex process of crack initiation, growth and fracture pattern formation. An understanding and accurate modeling of the fractural process is required for failure prediction. The stress and displacement fields near a crack-tip govern the fracture process that takes place at the crack-tip. Therefore, the study of these fields is vital for the fracture analysis. It has been difficult to model the region near a crack-tip by traditional methods due to existence of singularity nature. Generally a single parameter called stress intensity factors (SIFs) – coefficients of the singular term of the stress field – has been used to characterize fracture processes. However, recent studies show that constant and higher order non-singular terms of stress field are of great relevance in characterizing the fracture behaviors[1) - 6)] and hence the accurate and efficient numerical evaluation of these coefficients for cracked geometries have been receiving much attention over the last few years [4)].

In order to calculate these parameters of the stress field, researchers have proposed several analytical and numerical techniques. Since the analytical solutions for the fractural parameters are available only for a few idealized cases, numerical methods need to be employed for practical problems. Finite element method (FEM) and boundary element method (BEM) are the most popular numerical methods when rigorous solutions to realistic crack problems are sought. Unfortunately, these methods have some limitations and are inefficient to deal with crack problems. FEM's shortcoming is that its solution converges very slowly if conventional elements, that do not include stress singularities properly, are used. Tong and Pian [7)] have shown that, in general, the convergence rate of FEM solution is dominated by the nature of the singularities. They have also shown that regular high accuracy element (i.e using high order polynomials as interpolation functions) cannot improve the rate of convergence because the error from the elements immediately adjacent to the point of singularity is of the same order as that from the remainder of the elements. Therefore, the use of finer elements cannot improve the situation either. In order to improve the rate of convergence of the solution, considerable research has been directed towards developments of sophisticated mesh generation procedures or adaptive techniques such as hybrid crack element (HCE) method [8)], extended finite element method (XFEM) [9)], S-version FEM (s-FEM) [10)] and singular p-version FEM[11)]. On the other hand, BEM has certain

advantages over the domain-type method e.g. FEM and mesh-less method [12]; it reduces the problem size and the problem setup since it only needs boundary discretization of the studied problems. But the numerical implementation of BEM requires fundamental solution and advanced mathematical knowledge to deal with various singular integrals. Besides, the standard FEM and BEM are based on assumed piecewise smooth functions, which do not resemble the exact solution near the singular point [13].

A recently developed computational method, the scaled boundary finite element method (SBFEM) [14] is emerging as an alternative approach in order to overcome the deficiencies of FEM and BEM. It tries to combine the advantages of both FEM and BEM and avoids some of their drawbacks. As will be discussed later, SBFEM has a unique capacity to accurately compute stress and displacement field of singularities region at the crack-tip without any *a priori* assumptions; and it is not necessary to discretize the straight crack faces and faces ahead of the crack-tip when the so called 'scaling center' lies on the crack-tip.

Since SBFEM is a new method, the applications of the method are still unexplored in many fields, especially in the area of fracture mechanics. In this regards, Song & Wolf [15], and Deeks [16] have previously applied SBFEM to determine SIF in two-dimensional problems. Recently Song[17] has applied SBFEM to determine dynamic SIFs by using super elements. This paper extends the application of SBFEM for computing the elastic T-stress and higher order non-singular terms in two-dimensional fracture problems. In this paper a simple technique for these coefficients is presented by comparing the stress along the radial points ahead of the crack-tip with that of standard Williams' eigenfunction expansion of the linear elastic stress field at the crack-tip. The technique can be applied directly as well as independently to evaluate coefficients of the stress fields and has more advantages than other methods because of its simplicity in expression and less computational efforts in implementation.

2. Stress field near a crack-tip

The Williams' eigenfunction expansion[18] for crack-tip stress fields in any linear elastic body is given by a series of the form

$$\sigma_{ij}(r,\theta) = A_1 r^{-1/2} f_{ij}^{(1)}(\theta) + A_2 r^{0} f_{ij}^{(2)}(\theta) + \sum_{n=3}^{\infty} A_n r^{n/2} f_{ij}^{(n)}(\theta) \quad (1)$$

where (r, θ) are the local polar coordinates with the origin at the crack-tip, as shown in Fig. 1, the coefficients A_1, A_2 embodies SIFs and T-stress whose values vary with applied load and geometry of the cracked body, $f_{ij}(\theta)$ are the functions of θ, and A_n is the higher order coefficient term. The first term consisting of the inverse square root singular $r^{-1/2}$ component is referred to as the singular stress and the remaining terms, regular in the radial co-ordinate (r), are referred to as the non-singular stress.

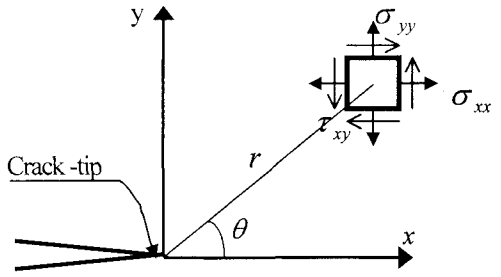

Fig. 1 *Stress fields near crack-tip*

According to Ref. [12], the asymptotic stress field for Mode I can be written as

$$\begin{Bmatrix} \sigma_x \\ \sigma_y \\ \tau_{xy} \end{Bmatrix} = \frac{K_I}{\sqrt{2\pi r}} \cos\left(\frac{\theta}{2}\right) \begin{Bmatrix} 1 - \sin\left(\frac{\theta}{2}\right)\sin\left(\frac{3\theta}{2}\right) \\ \sin\left(\frac{\theta}{2}\right)\cos\left(\frac{3\theta}{2}\right) \\ 1 + \sin\left(\frac{\theta}{2}\right)\sin\left(\frac{\theta}{2}\right) \end{Bmatrix} + \begin{Bmatrix} T \\ 0 \\ 0 \end{Bmatrix} + \sum_{n=3}^{\infty} A_n r^{n/2} \begin{Bmatrix} f_x^{(n)}(\theta) \\ f_y^{(n)}(\theta) \\ f_{xy}^{(n)}(\theta) \end{Bmatrix} \quad (2)$$

where K_I is the SIF for Mode I and T is the elastic T-stress. The Eq. (2) indicates that T-stress appears only in the σ_x component.

3. Scaled boundary finite element method

The scaled boundary finite element method is a new semi-analytical fundamental solution-less BEM based on FEM[14]. It is semi-analytical in the sense that it transforms the partial differential equation of a variety of linear problems into ordinary differential equations. These ordinary differential equations are solved analytically in radial direction and the coefficients of these equations are determined by the finite element approximation in the circumferential directions. The virtual work derivations of the stress and displacement fields in the method are presented in detail in Ref. [19] but are summarized here for convenience as follows

Governing equations of elastostatics

For two-dimensional elastostatics problems, the strains $\{\varepsilon(x, y)\}$ related to the displacement $\{u(x, y)\}$ by

$$\{\varepsilon(x,y)\} = \begin{Bmatrix} \varepsilon_x \\ \varepsilon_y \\ \gamma_{xy} \end{Bmatrix} = \begin{bmatrix} \partial/\partial x & 0 \\ 0 & \partial/\partial y \\ \partial/\partial y & \partial/\partial x \end{bmatrix} \begin{Bmatrix} u_x \\ u_y \end{Bmatrix} \quad (3)$$
$$= [L]\{u(x,y)\}$$

where $[L]$ is linear differential operator.

And the stresses $\{\sigma(x,y)\}=[\sigma_x, \sigma_y, \tau_{xy}]^T$ are given by

$$\{\sigma(x,y)\}=[D]\{\varepsilon(x,y)\}=[D][L]\{u(x,y)\} \tag{4}$$

with the elasticity matrix $[D]$

In no body load case, the internal equilibrium in elastostatics leads to the differential equation

$$[L]^T\{\sigma(x,y)\}=0 \tag{5}$$

which must be satisfied at every point within the domain.

Scaled boundary coordinate system

In this method, a coordinate system consists of a radial direction (ξ) and a local circumferential direction (η) is introduced (Fig. 2). The radial coordinate is defined to be zero at 'scaling center', and to have unit value on the boundary. The circumferential coordinate measures the distance anticlockwise around the boundary. The coordinate system is termed the scaled boundary coordinate system, and related to Cartesian coordinate by

$$x = x_0 + \xi\, x(\eta) \tag{6a}$$

$$y = y_0 + \xi\, y(\eta) \tag{6b}$$

where $x(\eta)$ and $y(\eta)$ are the functions describing the variation of the boundary in x and y directions as functions of η.

Applying standard procedures to transform the geometry from Cartesian co-ordinates to the scaled boundary co-ordinates defined in above Eq. (6), the linear operator in Eq. (3) can be written in the co-ordinate ξ, η as

$$[L]=[b^1(\eta)]\frac{\partial}{\partial\xi}+\frac{1}{\xi}[b^2(\eta)]\frac{\partial}{\partial\eta} \tag{7}$$

where $[b^1(\eta)]$ and $[b^2(\eta)]$ depend only on the geometry of the boundary.

Displacement function

The displacements at any point in the domain defined by scaled boundary coordinates (ξ, η) can be expressed in the form:

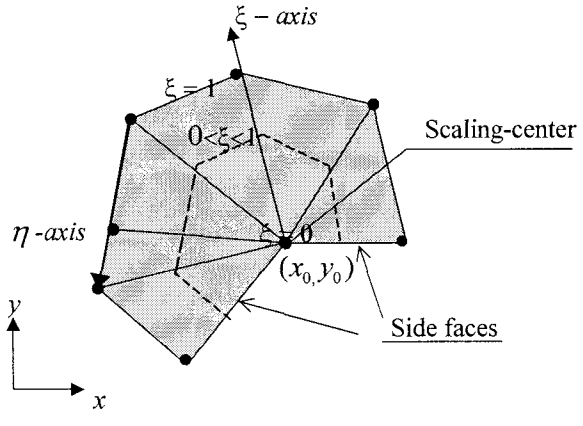

Fig. 2: *Scaled boundary coordinate system*

$$\{u(\xi,\eta)\}=\sum_{i=1}^{n}N_i(\eta)\{u_i(\xi)\}=[N(\eta)]\{u(\xi)\} \tag{8}$$

which represents a discretization of the boundary only.

Substituting Eqs. (7) and (8) in Eq. (5) lead to the approximate stresses in the co-ordinate ξ, η as

$$\{\sigma(\xi,\eta)\}=[D][B^1(\eta)]\{u(\xi)\}_{,\xi}+\frac{1}{\xi}[D][B^2(\eta)]\{u(\xi)\} \tag{9}$$

where

$$[B^1(\eta)]=[b^1(\eta)][N(\eta)]$$
$$[B^2(\eta)]=[b^2(\eta)][N(\eta)] \tag{10}$$

These results can be used in the virtual work equation to solve for the radial displacements.

Scaled boundary finite element equation

The virtual work statement is applied to introduce the equilibrium. When the domain is subjected to a set of boundary tractions $\{t\}$, the virtual work statement is

$$\int_V\{\delta\varepsilon\}^T\{\sigma\}dV=\int_S\{\delta u\}^T\{t\}ds \tag{11}$$

Performing integrals over the domain and then a series of mathematical manipulations, the virtual work statement is satisfied for all virtual displacements $\{\delta u(\xi)\}$ when

$$[E^0]\xi^2\{u(\xi)\}_{\xi\xi}+[[E^0]+[E^1]^T-[E^1]]\{u(\xi)\}_{\xi}-[E^2]\{u(\xi)\}=0 \tag{12}$$

where the coefficient matrices

$$[E^0]=\int_{-1}^{1}[B^1]^T[D][B^1]|J|d\eta \tag{13a}$$

$$[E^1]=\int_{-1}^{1}[B^2]^T[D][B^1]|J|d\eta \tag{13b}$$

$$[E^2]=\int_{-1}^{1}[B^2]^T[D][B^2]|J|d\eta \tag{13c}$$

are independent of ξ. The integrals of these $[E^0]$, $[E^1]$, and $[E^2]$ are evaluated using *Gaussian quadrature*. Eq. (12) is a standard ordinary differential equation for the displacements $u(\xi)$ with the dimensionless radial coordinate ξ as the independent variable.

Solution procedures

By inspection, solution to the set of Euler-Cauchy differential equation represented by Eq. (12) must be of the form

$$\{u_h(\xi)\}=\sum_{i=1}^{n}c_i\xi^{-\lambda_i}\{\phi_i\} \tag{14a}$$

where the exponents λ_i and vectors $\{\phi_i\}$ are interpreted as a radial scaling factor and a displacement modes shapes.

The displacements for each mode from Eq. (14a) can be written as

$$\{u(\xi,\eta)\}=\xi^{-\lambda}\{\phi\} \tag{14b}$$

Now substituting the Eq. (14b) and its derivations into Eq.

(12) and then simplifying yields the quadratic eigenproblem.

$$[\lambda^2[E^0]-\lambda[[E^1]^T-[E^1]]-[E^2]]\{\phi\}=\{0\} \tag{15}$$

This eigenproblem can be solved using standard techniques, yielding $2n$ displacement modes, where n is the number of nodes used in boundary discretization, and hence is also the size of the coefficient matrices.

Bounded problems can be represented conveniently by taking $0 \le \xi \le 1$. For such problems, only n modes with negative real component of λ lead to finite displacements at scaling center. This subset of n nodes is denoted by $[\Phi_1]$. For any set of boundary node displacements, u, the integration constants are

$$\{c\}=[\Phi_1]^{-1}\{u\} \tag{16}$$

The displacement fields can be obtained using

$$\{u(\xi,\eta)\}=[N(\eta)]\sum_{i=1}^{n}c_i\xi^{-\lambda_i}\{\phi_i\} \tag{17}$$

and the stress field is

$$\{\sigma(\xi,\eta)\}=[D]\sum_{i=1}^{n}[c_i\xi^{-\lambda_i-1}[-\lambda_i[B^1(\eta)]+[B^2(\eta)]]\{\phi_i\}] \tag{18}$$

Eqs. (17) and (18) are, respectively, the semi-analytical solutions for displacement and stress fields inside the domain.

4. SBFEM formulation for fractural parameters

In the numerical SBFEM analysis, it is already mentioned that the stress and displacement field along the radial direction emanating from the crack-tip where the stress singularity occur can be analytically calculated when the so called 'scaling center' is chosen at the crack-tip, as shown in the Fig. 3. In addition, only the boundaries, but not the straight crack faces and faces passing through the crack-tip, are discretized,

Now the stress field Eq. (18) can be expanded as

$$\begin{aligned}\sigma(\xi,\eta)&=A_1\xi^{-\frac{1}{2}}+A_2\xi^{0}+A_3\xi^{\frac{1}{2}}+\ldots+A_n\xi^{\frac{n}{2}-1}\\&=\sum_{i=1}^{n}A_i\xi^{\frac{i}{2}-1}\end{aligned} \tag{19}$$

where the coefficients $A_i=c_i\{\hat{\sigma}(\eta)\}_I$, $\hat{\sigma}(\eta)$ is the stress component that depend only on the circumferential coordinate η, and are constants for a given radial direction of a given element.

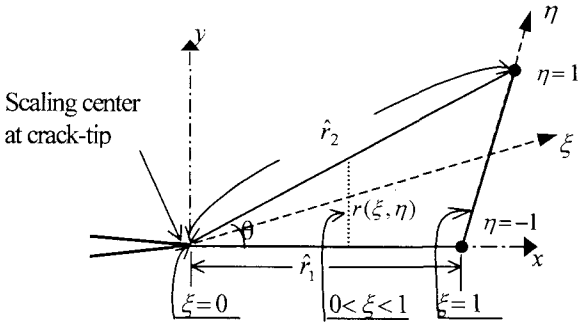

Fig. 3 SBFEM element with different coordinates

The stress components $\hat{\sigma}(\eta)$ are

$$\begin{aligned}\{\hat{\sigma}(\eta)\}&=\{\hat{\sigma}_x,\hat{\sigma}_y,\hat{\sigma}_{xy}\}^T\\&=[D][-\lambda[B^1(\eta)]+[B^2(\eta)]]\{\phi\}\end{aligned} \tag{20}$$

and the power of ξ is

$$\lambda_i=\frac{i}{2} \qquad \forall\ i=1,2,3,\ldots,n \tag{21}$$

For a given radial direction emanating from the crack-tip and inclined at an angle θ to the global x-axis as shown in Fig. (3), the following relationships are obtained from Eq. (6) as

$$r=r(\xi,\eta)=\xi\hat{r} \tag{22}$$

and

$$\tan\theta=\frac{y(\eta)}{x(\eta)} \tag{23}$$

where $\hat{r}=r(\eta)=\sqrt{x(\eta)^2+y(\eta)^2}$ are the radial distances of the boundary nodes from scaling center, and r is a distance measured from the crack-tip along the ray. The angle θ and the distance $\hat{r}$ are constants for a given radial direction of a given element.

After substituting the Eq. (22), the Eq. (19) becomes

$$\begin{aligned}\sigma(\xi,\eta)&=\{A_1\hat{r}^{\frac{1}{2}}\}r^{-\frac{1}{2}}+\{A_2r^0\}r^0\\&\quad+\{A_3\hat{r}^{-\frac{1}{2}}\}r^{\frac{1}{2}}+\ldots..+A_n\hat{r}^{\frac{n}{2}-1}\}r^{\frac{n}{2}-1}\\&=\sum_{i=0}^{n}A_i\hat{r}^{-\frac{i}{2}-1}r^{\frac{i}{2}-1}\end{aligned} \tag{24}$$

Eq. (24) is similar to Williams' expansion of the stress field, Eq. (1) at $\theta=0$. Thus, the stress intensity factors and T-stress and higher order coefficient terms of stress field near crack-tip can be computed by equating the coefficients of like powers of r terms of Eqs. (24) and (2) as follows.

Stress intensity factor for mode I is

$$K_I=c_i\hat{\sigma}_y\sqrt{2\pi\hat{r}} \tag{25}$$

T-stress is

$$T=c_i\hat{\sigma}_x \tag{26}$$

and higher order coefficients

$$a_n=c_nA_n\hat{r}^{-\frac{n}{2}-1} \qquad \forall\ n=1,2,3,\ldots \tag{27}$$

These equations (Eqs. (25)-(27)) indicate that SBFEM can be applied directly to evaluate the coefficients of singular, constant and higher order non-singular terms independently.

5. Numerical examples

In this section, the proposed SBFEM formulation was applied to perform fracture analysis, especially the analysis of stress field near crack-tip of a crack specimen. Only single loading (Mode I)

condition was considered and the following two fracture specimens with different geometry were simulated.

i) Single edge-crack tension (SECT) specimen, and

ii) Center-crack plate under tension (CCPT) specimen.

The analyses were carried out using plain strain condition with Young's modulus E = 1.0 and Poisson's ratio ν = 0.3. The applied load is σ_0 = 1 with its units consistent with that of E. Unit thickness was assumed. The specimens were subjected to a uniform remote tension, σ_0, at their ends. Only a half of SECT specimen and quarter of CCPT specimen (highlighted portions in schematic diagrams) were modeled by virtue of symmetry. The discretizations employed in this study consisted of three-node iso-parametric quadratic line elements on the boundary as shown in Fig 4. For the SBFEM calculation, only the stress along the radial line passing through first node ($\eta = -1$) of first element, as shown in Fig. 3, was calculated to approach the crack-tip along its line of propagation. The scaling center was placed at the crack-tip in SBFEM mesh and, therefore, the straight crack face and the face ahead of the crack-tip were not discretized.

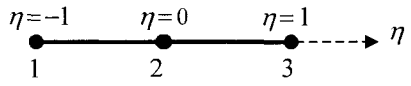

Fig. 4 Three-node line finite element

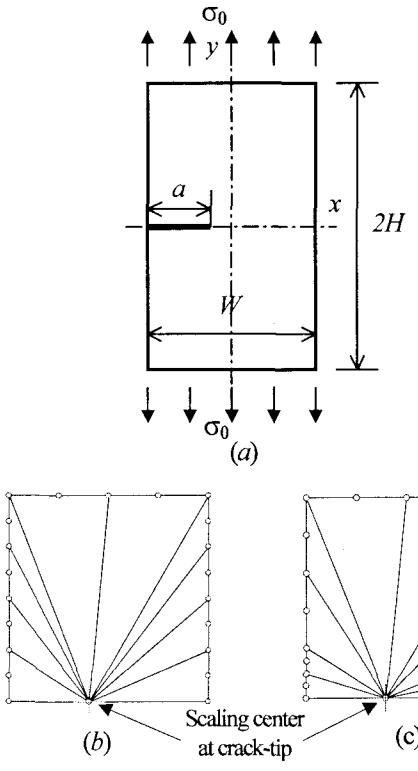

Fig. 5 (*a*) Schematic diagram for SECT, (*b*) *Mesh I*: uniform mesh, and (*c*) *Mesh II*: fine mesh near crack

5.1 Test of convergence

To examine the accuracy of the proposed SBFEM techniques, first the convergences of the calculation were checked considering the first specimen, SECT. The schematic diagram of the specimen is as shown in Fig 5 (*a*). Two different mesh patterns were considered.

i) Mesh I: uniform mesh

ii) Mesh II: fine mesh near crack

In the first mesh pattern called *Mesh I* in this paper, the discretization is uniform on all the discretized boundaries and in second mesh pattern, *Mesh II*, the discretization is finer near the crack area compared to other areas, as shown in Fig. 5 (*b*) and (*c*), respectively. To check the convergence of these mesh patterns, each mesh pattern was refined into four different meshes (coarse, medium, fine and very fine) by doubling the number of elements in each level of refinement. The coarse, medium, fine and very fine meshes consist of 5, 10, 20 and 40 elements with 22, 42, 82 and 162 degree of freedoms (DOFs), respectively. The medium mesh in each mesh patterns, with a/W = 0.4 and H/W = 1, are as shown in Fig. 5 (b) and (c). The scaling centers, i.e., the plus sign in the figures, are at the crack-tip. The crack faces and faces ahead of crack-tip were not discretized. The convergence of computed normalized SIF, $K_I/\sigma_0(\pi a)^{1/2}$, and normalized T-stress, $T(\pi a)^{1/2}/K_I$, of these mesh patterns for SECT with a/W = 0.4 and H/W = 1.0, are presented in Fig. 6 (*a*) and (*b*), respectively. The target values from Ref. [20] were 2.106 for normalized SIF and -0.27 for normalized *T*-stress. The figures clearly show that *Mesh II* gives better convergence results compared with *Mesh I*. In

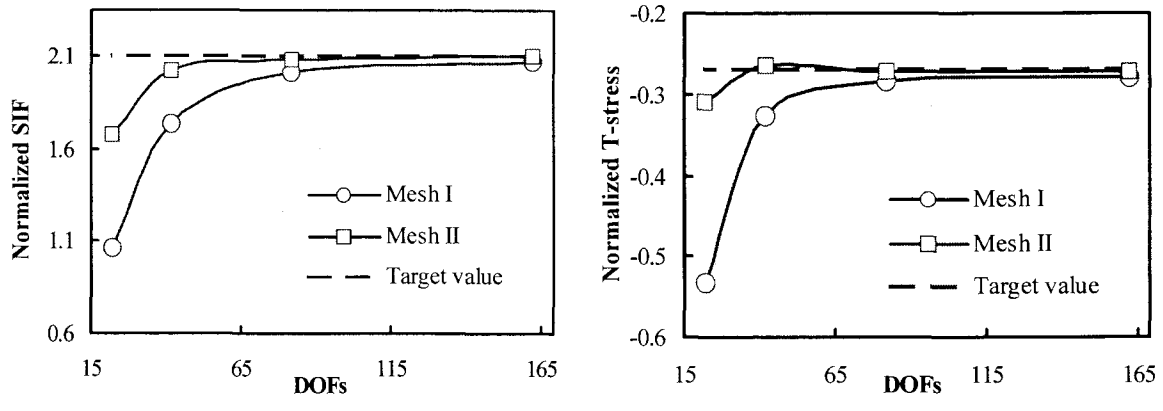

Fig. 6 Convergence of (*a*) normalized SIF and (b) normalized T-stress in *Mesh I* and *Mesh II* for SECT with a/W = 0.4 and H/W = 1.0

addition, the differences between the results of fine and very fine meshes are comparatively very less (less than 1%.) than that of other meshes. Therefore, *Mesh II* with very fine discretization was considered for further analysis. However, it should be mentioned that a formal convergence study was not carried out; this will be part of a more detailed investigation of the subjects in the future.

The computational time (CPU time) of the method for *Mesh II* with very fine mesh was less than 4 seconds on a Pentium IV 2.40 GHz PC. The CPU time includes times for the modeling, stiffness matrices computation and stress calculation; each taking 1.5%, 96% and 2.5% of total CPU time, respectively. However, the computational time of the SBFEM in solving the numerical examples are not compared with those of other method because Refs.[21-22] has demonstrated that the SBFEM out-performs the FEM in situations involving stress concentrations or unbounded domains, reducing significantly the program run-time for the same accuracy.

5.2 Accuracy of the proposed method

In this section, the stress along y-direction σ_y ahead of the crack-tip for CCPT and the coefficients, $a_n (1 \le n \le 9)$, of the asymptotic fields near the crack-tip for both SENT and CCPT were evaluated by using Eq. (18) and the proposed SBFEM formulations (Eqs (25) – (27)), respectively. The first analysis i.e., computation of near tip stress was considered to demonstrate the accuracy and efficiency of SBFEM compared with FEM, and the second analysis was considered to verify the validity of the proposed formulation.

(1) Stress ahead of crack-tip

A center crack plate under tension (CCPT) was considered to analyze the stress ahead of a crack-tip. The schematic diagram of the problem is as shown in Fig. 7 (*a*), where H and W are plate dimensions and a is the crack length. The geometrical parameters used for the analysis were $a = 1$, $W = 2$, and $H = 4$. The objective was to predict the near tip stress σ_y by the present method, SBFEM, and compare with the corresponding FEM to verify the accuracy and efficiency of SBFEM.

The SBFEM analysis was performed with single discretization of 42 DOFs (21 nodes), as shown in Fig. 7 (c). The FEM analysis was performed with three different discretizations - coarse of 90 DOFs (45 nodes), medium of 366 DOFs (183 nodes) and fine of 1260 DOFs (630 nodes). The FEM fine mesh is as shown in Fig. 7 (b). Fig. 8 presents the plots of computed stress σ_y normalized by applied stress σ_0 (σ_y/σ_0) as a function of $x/(W-a)$. The computed SBFEM results of 42 DOFs were compared with those of three different FEM results with increasing number of DOFs from 90 to 1260. Fig. 8 shows close agreement of all the computed results except in the region near

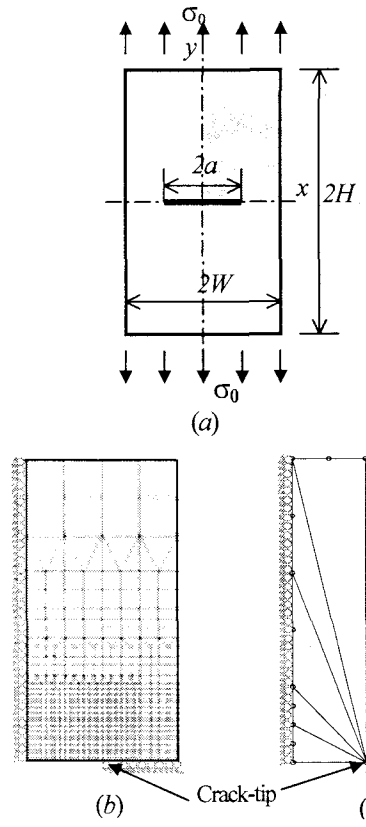

Fig. 7 (*a*) Schematic diagram for CCPT, (b) fine FEM mesh with 1260 DOFs, and (c) SBFEM mesh with 42 DOFs

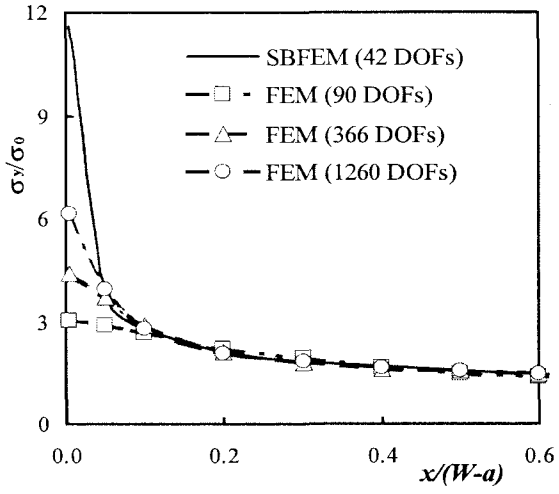

Fig. 8 Stress along y-direction, σ_y, ahead of crack-tip

crack-tip where singularity occurs. In the singularity region, singularity of FEM results increase with increase in mesh size, but SBFEM results, with less than 4% DOFs of fine-mesh FEM, show more singularity than FEM results.

(2) Computation of singular and higher order terms

To compute the SIFs, T-stress and higher order terms, both SECT and CCPT specimens were analyzed for a range of crack-sizes. The geometrical parameters $W = H = 4$ and tensile stress $\sigma_0 = 1$ for both problems were considered for analysis. As

Table 1 Coefficients, a_n ($1 \le n \le 9$) in Eq. (27) of the asymptotic stress field near the crack-tip for SECT.

Coefficient	Power of ξ			Coefficients			Ratio*	
a_i	SBFEM	Exact	Error %	SBFEM	BCM [23]	HCE [23]	BCM	HCF
a_1	-0.5000	-0.5000	0.00	1.0593	1.0794	1.0585	0.98	1.00
a_2	2.98×10^{-13}	0.0000	0.00	-0.1505	-0.1135	-0.1513	1.33	0.99
a_3	0.5000	0.5000	0.00	0.0795	0.0656	0.0815	1.21	0.98
a_4	1.0000	1.0000	0.00	-0.0475	-0.0367	-0.0478	1.29	0.99
a_5	1.4999	1.5000	-0.01	0.0056	-0.0057	0.0055	-0.98	1.02
a_6	1.9999	2.0000	0.00	0.0233	–	–	–	–
a_7	2.5012	2.5000	0.05	0.0181	–	–	–	–
a_8	3.0023	3.0000	0.08	-0.0078	–	–	–	–
a_9	3.5029	3.5000	0.08	0.0118	–	–	–	–

* Ratio = computed SBFEM value/ reference value

explained above, the convergences of the calculation were examined with four different mesh refinements (coarse, medium, fine and very fine) for both problems. It generally shows that the convergence of the first three terms is very rapid compared with the last two terms. The computed results of the first–ninth coefficient terms of the stress fields of very fine mesh of 40 elements with 81 nodes are presented in Tables 1 and 2 for SECT and CCPT, respectively, with corresponding eigenvalues (power of ξ i.e., $-\lambda-1$). Both the Tables show that the first-fourth computed power are in good agreement with the actual values, but the power terms for higher order coefficients deviated from actual values which indicated that further refinement is necessary for higher order terms. The computed SBFEM coefficients were compared with HCE and Boundary Collocation Method (BCM) results from Ref. [24) and 25)]. In the reference literatures, a 9-node HCE together with 112 quadrilateral elements giving a total of 137 nodes are used for the analysis of CCPT specimen and 21-node HCE with p–adaptivity are used for SECT specimen analysis. Tables 1 and 2 show that the SBFEM coefficient results of SECT agree very well with the HCE solution compared with BCM and that of CCPT specimen is very close to that of BCM (less than 0.4% derivation). Karihaloo et al.[23] has recommended HCE method for SECT analysis, but Xiao et al. [24] mentions that the n-node polygonal HCE method predicts wrong results for coefficients corresponding to higher order terms in Mode I and Mode II, and recommended BCM for CCPT analysis. The agreement of the result obtained by the SBFEM formulation was an excellent with that of recommended method in literatures.

The tables also include computed SBFEM results of 6th to 9th coefficients for both SECT and CCPT specimens. As per the authors' knowledge, none of the previous studies have addressed the computations of these coefficients.

6. Conclusion

The coefficients, not only singular term (SIFs) but also the constant (T-stress) and the higher order non-singular terms of the asymptotic fields near crack-tip of a cracked body can be directly calculated using a recently developed semi - analytical method, called scaled boundary finite element method. A simple and

Table 2 Coefficients, a_n ($1 \le n \le 9$) in Eq. (27), of the asymptotic stress field near the crack-tip for CCPT

Coefficient	Power of ξ			Coefficients			Ratio*	
a_i	SBFEM	Exact	Error %	SBFEM	BCM [24]	HCE [24]	BCM	HCF
a_1	-0.5000	-0.5000	0.00	0.7674	0.7680	0.7665	1.00	1.00
a_2	1.52×10^{-13}	0.0000	0.00	-0.2774	-0.2777	-0.2779	1.00	1.00
a_3	0.5000	0.5000	0.00	0.1865	0.1866	0.1915	1.00	0.97
a_4	1.0000	1.0000	0.00	0.0030	0.0030	-0.0018	1.00	-1.67
a_5	1.4999	1.5000	-0.01	-0.0278	-0.0279	-0.0235	1.00	1.18
a_6	1.9998	2.0000	-0.01	0.0008	–	–	–	–
a_7	2.5014	2.5000	0.06	0.0057	–	–	–	–
a_8	3.0023	3.0000	0.08	-0.0001	–	–	–	–
a_9	3.5035	3.5000	0.10	-0.0018	–	–	–	–

* Ratio = computed SBFEM value/ reference value

direct formulation was derived for evaluating these coefficients of the stress field by comparing the classical linear elastic field solution in the vicinity of a crack-tip to that of SBFEM after power series expansion. The validity of these formulations were examined with two example problems for a range of crack sizes, with good agreement obtained between the SBFEM results and the corresponding ones in the literature. Based on the results of the study it can be confirmed that the proposed numerical method can be applied to crack problems more easily with relatively coarse and simple model than other computational methods.

This paper dealt with simple two-dimensional bounded problems with single crack under single loading (Mode I) condition. The present method can be applied into complex geometry, multi-cracks, and mixed mode condition problems by extending the present approach. Moreover, it can be extended into three-dimensional, unbounded and dynamic problems. In the three-dimensional and unbounded problems, the advantages of reducing modeling tasks would be more pronounced than in two-dimensional cases.

REFERENCES

1) Larsson, S. G, and Carlsson A. J., Influence of non-singular stress terms and specimen geometry on the small-scale yielding at crack-tip in elasto-plastic material, *J Mech Phys Solids*, 21, pp 263-77, 1973
2) Du Z. Z. and Hancock J.W., The effect of non-singular stresses on crack-tip constraint. *J Mech Phys Solids*, 39, pp 555-67, 1991
3) Dyskin, A.V., Crack growth criteria incorporating non-singular stresses: Size effects in apparent fracture toughness, *International Journal of Fracture*, 83, pp 191-206, 1997.
4) Karihaloo, B. L. and Xias, Q. Z., Accurate determination of the coefficients of elastic crack-tip asymptotic field by a hybrid crack elements with *p*-adaptivity, *Engineering Fracture Mechanics*, 68, pp 1609-1630, 2001.
5) Yang, S., Chao, Y. J. and Sutton M. A., Higher order asymptotic crack-tip fields in a power-law hardening materials *Engineering Fracture Mechanics*, 45, pp 1-20, 1993.
6) Jeon, I. and Im, S., The role of higher orders eigenfields in elastic-plastic cracks, *J Mech Phys Solids*, 49, pp 2789-2818, 2001.
7) Tong P., Pian T. H. H., On the convergence of the finite element method for problems with singularity. *International Journal of Solids and Structures*, 9, pp 313-321, 1973.
8) Tong, P., Pian, T. H. H. and Lasry, S. J., A hybrid element approach to crack problems in plane elasticity. *Int. J. Num. Meth. Engg*, 7, pp 297-308, 1973.
9) Nagashima, T, Omoto, Y. and Tani, S., Stress intensity factor analysis of interface cracks using X-FEM, *Int. J. Num. Meth. Engg.*, 56, pp 1151-1173, 2003.
10) Hiroshi O., Sayaka E. and Masanori K., On fracture analysis using an element overlay technique, *Engineering Fracture Mechanics*, 68, pp 1609-1630, 2005.
11) Rahaulkumar, P., Saigal, S. and Yunus, S., Singular p-version finite elements for stress intensity factor computations, *Int. J. Num. Meth. Engg.*, 40, pp 1091-1114, 1997.
12) Sutradhar, A. and Paulino, G. H., Symmetric Galerkin boundary finite element computation of T-stress and SIFs for mixed-mode cracks by the interaction in integral method, *Engineering Analysis with Boundary Elements.* 28, pp 1335–1350, 2004.
13) Oh H. S., Babuska I., The *p*-version of the finite element method for the elliptic boundary value problems with interfaces. *Computer Methods in Applied Mechanics and Engineering.* 97, 211-231, 1992.
14) Wolf J.P., *The Scaled Boundary Finite Element Method*: John Wiley & Sons Ltd, 2003.
15) Song, C., Wolf J. P., Semi-analytical representation of stress singularity as occurring in cracks in anisotropic multi-materials with the scaled boundary finite-element method. *Computers and Structures*, 80, pp 183-197, 2002.
16) Deeks, A. J., Calculation of stress-intensity factors using the scaled boundary finite-element method. *Proc. Int. Conf. Struct. Integrity and Fracture*, Perth, pp 3-8, 2002.
17) Song C., A super-element for crack analysis in the time domain. *Int. J. Num. Meth. Engg*, 61, pp 1332-57, 2004.
18) Williams M. L. On the stress distribution at the base of a stationary crack, *J Appl Mech, ASME*, 24, pp109-14, 1957.
19) Deeks. A. J. and Wolf, J.P., A virtual work derivation of the scaled boundary finite element method for elastostatic, *Computational Mechanics*, 28, pp 489-509, 2002.
20) Yang B., Ravi-Chandar K., Evaluation of elastic T-stress by stress difference method. *Engineering Fracture Mechanics,* 64, pp 589-605, 1999.
21) Deeks, A. J. and Wolf, J. P., Stress recovery and error estimation for the scaled boundary finite-element method. *J. Num. Meth. Engg,* 54(4), pp 557–583, 2002
22) Deeks A.J. and Wolf J. P., An h-hierarchical adaptive procedure for the scaled boundary finite-element method. *Int. J. Num. Meth. Engg*, 54, pp 585-605, 2002.
23) Karihaloo, B. L. and Xias, Q. Z., Approximate Green's functions for singular and higher order terms of an edge crack in a finite plate, *Engineering Fracture Mechanics*, 69, pp 959-981, 2002.
24) Xias, Q. Z., Karihaloo, B. L. and Liu, X.Y., Direct determination of SIF and higher order terms of mixed mode cracks by a hybrid crack element. *International Journal of Fracture*, 125, pp 207-225, 2004.

(Received April 15, 2005)